

Annual Review of Physical Chemistry
Molecular Simulations of
Gram-Negative Bacterial
Membranes Come of Age

Wonpil Im^{1,2} and Syma Khalid³

¹Departments of Biological Sciences and Bioengineering, Lehigh University, Bethlehem, Pennsylvania 18015, USA; email: wonpil@lehigh.edu

²School of Computational Sciences, Korea Institute for Advanced Study, Seoul 02455, Republic of Korea

³School of Chemistry, University of Southampton, Southampton S017 1BJ, United Kingdom; email: S.Khalid@soton.ac.uk

Annu. Rev. Phys. Chem. 2020. 71:171–88

First published as a Review in Advance on
February 18, 2020

The *Annual Review of Physical Chemistry* is online at
[physchem.annualreviews.org](https://www.annualreviews.org)

<https://doi.org/10.1146/annurev-physchem-103019-033434>

Copyright © 2020 by Annual Reviews.
All rights reserved

Keywords

bacterial membranes, lipopolysaccharide, cell envelope, atomistic, coarse-grained, membrane proteins, O-antigen

Abstract

Gram-negative bacteria are protected by a multicompartamental molecular architecture known as the cell envelope that contains two membranes and a thin cell wall. As the cell envelope controls influx and efflux of molecular species, in recent years both experimental and computational studies of such architectures have seen a resurgence due to the implications for antibiotic development. In this article we review recent progress in molecular simulations of bacterial membranes. We show that enormous progress has been made in terms of the lipidic and protein compositions of bacterial systems. The simulations have moved away from the traditional setup of one protein surrounded by a large patch of the same lipid type toward a more biologically representative viewpoint. Simulations with multiple cell envelope components are also emerging. We review some of the key method developments that have facilitated recent progress, discuss some current limitations, and offer a perspective on future directions.

ANNUAL
REVIEWS **CONNECT**

www.annualreviews.org

- Download figures
- Navigate cited references
- Keyword search
- Explore related articles
- Share via email or social media

INTRODUCTION

Antimicrobial resistance is a phrase that is now universally familiar due to the recent mainstream media attention on this topic, prompted by the huge threat posed by such resistance to human, animal, and plant life. If antibiotic drug development continues at the current pace, one recent projection has estimated that by the year 2050 more patients will die from bacterial infections than from cancer, with costs approaching \$100 trillion (1). Bacteria are relatively simple organisms, certainly compared to eukaryotes. Yet the membranes that protect them are anything but simple, and indeed the complexity and adaptability of these membranes are key factors contributing to the development of bacterial resistance to antibiotics. To develop new and more potent antibiotics, we must first develop a thorough molecular-level understanding of the mechanisms by which bacteria protect themselves. To this end, there has been a recent resurgence in experimental and simulation studies aiming to understand the structure–function relationships of bacterial cell envelopes. Here we review progress in simulations of these bacterial cell envelopes over the last 5 years or so. To facilitate the reader’s understanding, we begin with a reminder of the structural and chemical details of the molecular architectures of bacterial cell envelopes.

Gram-negative and Gram-positive bacteria can be differentiated by the compositions of their cell envelopes. The former are characterized by a thin peptidoglycan cell wall that lies in the periplasm between the two (inner and outer) membranes (2). In contrast, Gram-positive bacteria have a much thicker cell wall (e.g., 30–100 nm) (3), which faces the external environment and contains only one membrane, which is located between the cell wall and the cytoplasm. While the fine details of the membrane compositions of the two types of bacteria are species dependent, some generalities do exist. The compositions of the two membranes of Gram-negative bacteria differ in that the inner membrane (IM) is essentially a symmetric bilayer composed of a mixture of phospholipids, whereas the outer membrane (OM) is asymmetric in that the outer leaflet contains lipopolysaccharide (LPS) molecules exclusively, whereas the inner leaflet contains phospholipids similar in composition to those of the IM. In Gram-positive bacteria, the membranes contain phospholipids in both leaflets, but often some of these lipids have larger, more complex headgroups than simple phospholipids, e.g., lysyl phosphatidylglycerol (PG) lipids in *Staphylococcus aureus*. Here we provide a summary of major progress in the molecular modeling and simulation field that has produced models of complex Gram-negative bacterial membranes beyond simple homogenous lipid bilayers that incorporate one or two proteins.

SIMULATING THE OUTER MEMBRANE

Perhaps the most significant impediment to studies of even minimal OMs of viable Gram-negative bacteria is the parameterization of LPS. An LPS molecule is a complex amphipathic compound consisting of a phylogenetically conserved lipid A, an (inner and outer) core oligosaccharide, and highly diverse O-antigen polysaccharides with various lengths of repeating units (up to ~100) that determine the bacterium’s antigenic diversity (4, 5). **Figure 1** shows some LPS chemical structures of *Pseudomonas aeruginosa* with three different core and O-antigen structures. Clearly, the heterogeneity of core structures, as well as O-antigen sequence diversity and repeating unit length, can create dynamic protein–LPS and LPS–LPS interactions.

Simulation studies of the OM that incorporate detailed models have tended to focus on *Escherichia coli* and *P. aeruginosa*, although more recent studies of the OMs of other species are appearing in the literature (**Table 1**). The first LPS model used in a membrane simulation study was from *P. aeruginosa* by Lins & Straatsma (6) in 2001. This model employed the Amber force field and incorporated Ra-LPS (with a full core only; it is also called the rough LPS). Later models of LPS

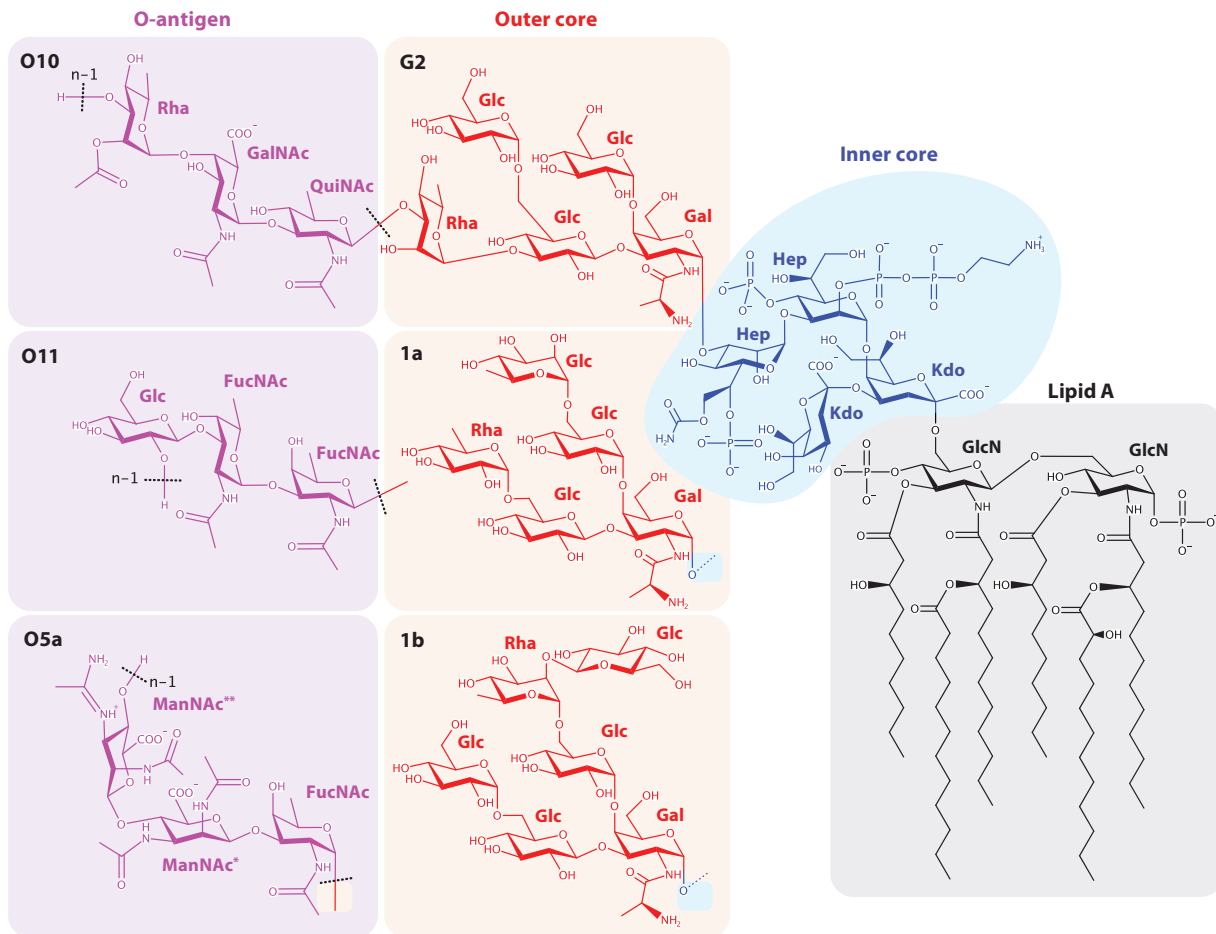


Figure 1

Chemical structures of *Pseudomonas aeruginosa* lipopolysaccharide. Note that the cores 1a and 1b cannot have any O-antigen attached to them, but the G2 core can. Three O-antigen structures (O10, O11, and O5a) are shown as examples. Abbreviations: FucNAc, *N*-acetyl-L-fucosamine; Gal, D-galactose; GalNAc, *N*-acetyl-D-galactosamine; Glc, D-glucose; GlcN, D-glucosamine; Hep, L-glycero-D-manno-heptose; Kdo, 2-keto-3-deoxyoctulosonate; ManNAc*, *N*-acetyl-D-mannosamine; ManNAc**, *N*-acetamidine-D-mannosamine; QuiNAc, *N*-acetyl-D-quinovosamine; Rha, L-rhamnose.

from *E. coli* using the GROMOS and CHARMM force fields were reported by the Khalid group (7) and the Im group (8, 9), respectively. Notably, the latter also incorporated the O-antigen component (i.e., smooth LPS) for the first time. Both *E. coli* models incorporated a realistic mixture of phospholipids in the inner leaflet.

A major practical breakthrough in constructing bacterial OM models has been the advent of automated membrane construction tools, of which the most popular and versatile is *LPS Modeler* (10) and its incorporation into *Membrane Builder* (11) in CHARMM-GUI (<http://www.charmm-gui.org>) (12) from the Im group. This tool features LPSs from 15 bacterial species and incorporates 37 lipid A, 52 core, and 305 O-antigen types. Prior to the release of LPS-containing *Membrane Builder*, few laboratories had the expertise to build complex Gram-negative bacterial OM systems containing LPS reliably and systematically. Indeed, it took approximately 6 months to correctly construct the first smooth LPS model from *E. coli* (W. Im, unpublished observation). In contrast,

Table 1 A summary of the literature of lipopolysaccharide models and outer membrane simulations

Year	Bacterial species	Membrane type	Level of detail	Force field	Reference
1999	<i>Escherichia coli</i>	One layer	AA	GLYCAM	16
2007	<i>Pseudomonas aeruginosa</i>	Asymmetric	AA	AMBER96&GLYCAM93	17
2008	<i>P. aeruginosa</i>	Asymmetric	AA	AMBER96&GLYCAM93	18
	<i>P. aeruginosa</i>	Asymmetric	AA	AMBER96&GLYCAM93	19
	<i>P. aeruginosa</i>	Asymmetric	AA	NWChem	20
2011	<i>E. coli</i>	Asymmetric	AA	GROMOS53A6	7
2012	<i>P. aeruginosa</i>	Asymmetric	AA	GLYCAM06	21
2013	<i>E. coli</i>	Asymmetric	AA	CHARMM36	8
2015	<i>P. aeruginosa</i>	Asymmetric	CG	Martini	22
	<i>P. aeruginosa</i>	Asymmetric	CG/AA	Martini/GROMOS	23
2016	Various bacteria	Symmetric	AA	CHARMM36	24
2017	<i>E. coli</i>	Asymmetric	AA	CHARMM36	25
	<i>E. coli</i>	Asymmetric	CG	Martini	14
	Various bacteria	Asymmetric	CG	Martini	26
2018	<i>P. aeruginosa</i>	Asymmetric	AA	GLYCAM06&Slipids	27
2019	<i>Campylobacter jejuni</i>	Asymmetric	AA	CHARMM36	10
	<i>E. coli</i>	Asymmetric	AA	CHARMM36	28
	<i>E. coli</i>	Asymmetric/ symmetric	CG/AA	Martini/CHARMM	29
	<i>Moraxella catarrhalis</i>	Symmetric	AA	CHARMM36	30

Abbreviations: AA, all-atom; CG, coarse-grained.

it takes about 5–10 minutes to build an LPS structure from various bacteria in *LPS Modeler*, and within minutes to a few hours, depending on the system size, to construct a membrane incorporating this structure in *Membrane Builder*. In addition, *Martini Maker* (13, 14) in CHARMM-GUI can be used to build various OMs using coarse-grained (CG) LPS models based on the Martini force field.

The number of atomistic and CG models of LPS has now grown. **Table 1** provides a summary of such models that have been reported to date (to the best of our knowledge). Rather than discussing the historical aspects of the development of these models, which can be found elsewhere (15), here we focus on the biophysical insights that have resulted from molecular simulations with these models.

An intriguing aspect of the stability of LPS-containing membranes is the role played by divalent cations. The importance of divalent cations has been highlighted by studies using all major force fields and has also been shown experimentally. The first mention of lipid A headgroups cross-linked by divalent cations was from simulations done by Lins & Straatsma (6), which are rather short by current standards. Nevertheless, the Khalid group (7) and the Im group (8, 9) in their studies using different force fields and longer simulations reported the same behavior. Divalent cations formed long-lived electrostatic interactions with phosphate moieties of LPS (**Figure 1**), and indeed did so simultaneously with phosphate groups from multiple LPS molecules, thereby forming an extended network of interactions across the headgroup region of the outer leaflet of the OM. This contributes to slow diffusion rates of LPS. The simulation studies, in agreement with experimental data, showed that LPS diffusion occurred at a rate that is an order of magnitude slower than that of phospholipids (7, 24). This is also likely a consequence, in part, of the greater number of lipid tails in LPS and the sheer bulk of the sugars. Thus, LPS diffuses slowly due to

having headgroups that are tightly cross-linked by divalent cations, between four to eight hydrocarbon tails, and multiple sugar groups. Recently, Hughes et al. (28) combined neutron reflectometry and molecular simulation to explore the physical properties of OM mimetics. They found excellent agreement between experiment and simulation, allowing experimental testing of the conclusions from simulations studies, and also atomistic interpretation of the behavior of experimental model systems, such as the degree of lipid asymmetry, the lipid component (tail, head, and sugar) profiles along the bilayer normal, and lateral packing (i.e., average surface area per lipid). Therefore, the combination of both experimental and simulation approaches continues to provide a powerful new means to explore the biological and biophysical behavior of the bacterial OM.

The importance of protein–membrane interactions in modulating and regulating the behavior of membrane proteins has been known for some time now. Development of the LPS models discussed above allowed the study of such interactions in the OM of Gram-negative bacteria. Here we discuss only a few selected case studies due to space limitations, but **Table 2** provides

Table 2 A summary of the literature on simulation studies of outer membrane proteins in outer membrane environments

Year	Protein(s)	Bacterial species	Level of detail	Reference
2009	OprF	<i>Pseudomonas aeruginosa</i>	AA	31
2013	FecA	<i>Escherichia coli</i>	AA	32
	Hia	<i>Haemophilus influenzae</i>	AA	33
2014	OmpLA	<i>E. coli</i>	AA	34
2015	OccD1	<i>P. aeruginosa</i>	CG	23
	Polymyxin B1	<i>E. coli</i>	AA	35
2016	BamA	<i>E. coli</i>	AA	36
	BtuB	<i>E. coli</i>	AA	37
	OmpA	<i>E. coli</i>	AA	38
	OmpA	<i>E. coli</i>	AA	39
	OmpF	<i>E. coli</i>	AA	40
2017	AcrABZ-TolC/OmpA	<i>E. coli</i>	CG	41
	OmpF	<i>E. coli</i>	AA	15
	OprH	<i>P. aeruginosa</i>	AA	42
	OmpA/OmpF	<i>E. coli</i>	CG	14
	Polymyxin B1	<i>E. coli</i>	CG	43
	PorB	<i>Neisseria gonorrhoeae</i>	AA	44
2018	Aquaporin Z, OmpF	<i>E. coli</i>	AA	45
	Occk5	<i>P. aeruginosa</i>	AA	46
	OmpA/OmpF	<i>E. coli</i>	CG	47
	OmpF	<i>E. coli</i>	CG	48
2019	BtuB	<i>E. coli</i>	AA	10
	OmpF	<i>E. coli</i>	AA	29
	OmpE36	<i>E. coli</i>	AA	49
	OmpA/OmpX/OmpF/ FhuA/EstA/BtuB	<i>E. coli</i>	CG	50
	OprD	<i>E. coli</i>	AA	51

Abbreviations: AA, all-atom; CG, coarse-grained.

a summary of all simulation studies of outer membrane proteins (OMPs) in OM models (to the best of our knowledge).

Rather frustratingly, there are only three structures of OMPs in complex with LPS in the Protein Data Bank (PDB): BtuB [PDB ID 1UJW; *E. coli* vitamin B12 (cyanocobalamin) transporter], FhuA (PDB ID 1QJQ; *E. coli* ferric hydroxamate receptor), and OmpE36 (PDB ID 5FVN; a major porin from *Enterobacter cloacae*). This paucity of experimental structural data requires molecular simulations to provide an in-depth and unprecedented understanding of interactions between the OMPs and OMs. One of the first studies of LPS interactions with an OMP from *E. coli* was reported by Khalid and colleagues (32). They showed that the large loops of FecA, which is a TonB-dependent transporter, interacted with various moieties of LPS, providing evidence that considering these OMPs in simple phospholipid bilayers is not likely to provide an accurate, realistic description of the conformational dynamics of the OMP loops. BtuB, another TonB-dependent transporter from *E. coli*, was studied by Balusek & Gumbart (37). In agreement with the aforementioned simulations of FecA, the extracellular loops of BtuB were also found to be stabilized to some extent through interactions with LPS. This finding suggests that these interactions may eliminate the need for Ca^{2+} binding. However, Ca^{2+} was also observed to play a role in stabilizing both the substrate-binding region and the apoprotein, facilitating rearrangement of the substrate-binding residues into a conformation that closely resembles that of the substrate-bound protein. Thus, while these simulations of TonB-dependent transporters were rather short by today's standards, they did emphasize the importance of including LPS in models of the OM when exploring the in vivo behavior of these proteins.

Lee et al. (42) explored the influence of various *P. aeruginosa* and *E. coli* LPS environments on the physical properties of OprH (outer membrane protein H of *P. aeruginosa*) using all-atom molecular simulations. Although the *P. aeruginosa* OMs are thinner hydrophobic bilayers than the *E. coli* OMs, which is expected from the difference in the acyl chain length of their lipid A, the simulations revealed that this effect is almost imperceptible around OprH due to a dynamically adjusted hydrophobic match between OprH and the OM (**Figure 2**). Consistent with previous experimental findings, calculated interaction patterns identified key residues for interactions between OprH and LPS. As it is difficult to determine well-defined orientations of the OprH loops by solution NMR experiments in detergent micelles, this study also illustrated that OprH-OM simulations could provide a general approach to refining functionally important loop conformations of OMPs. Recently, Kleinekathöfer and colleagues (49) investigated the geometric properties of the first LPS shell and the role of Ca^{2+} in LPS binding to OmpE36. The simulations reproduced LPS binding to OmpE36 in a recently determined crystal structure, but LPS binding in the simulations was not as compact as in the crystal structure. Their findings highlight the role of divalent cations in stabilizing the binding between proteins and LPS molecules in the OM of Gram-negative bacteria.

Kleinekathöfer and colleagues have reported several studies of OMPs in phospholipid bilayers to complement the experimental work of Winterhalter and colleagues (e.g., see 52, 53). More recently, the Kleinekathöfer group teamed up with the Im group to study the Occk5 channel from *P. aeruginosa* in various LPS-containing model OMs (46). The simulations revealed that Occk5 has a remarkable anion selectivity independent of both the OM composition and effective cation concentration. The entrance of Occk5 was found to be occluded by the outer core and O-antigens of LPS, which resulted in lowered diffusion constants of ions approaching the channel, and again served to reinforce that LPS-containing membranes cannot be neglected when considering the functioning of OMPs in their native membrane environments.

Free-energy calculations are notoriously expensive and are even more so when slow-moving LPS is considered. Nevertheless, characterizing energetics is a crucial aspect of the physical

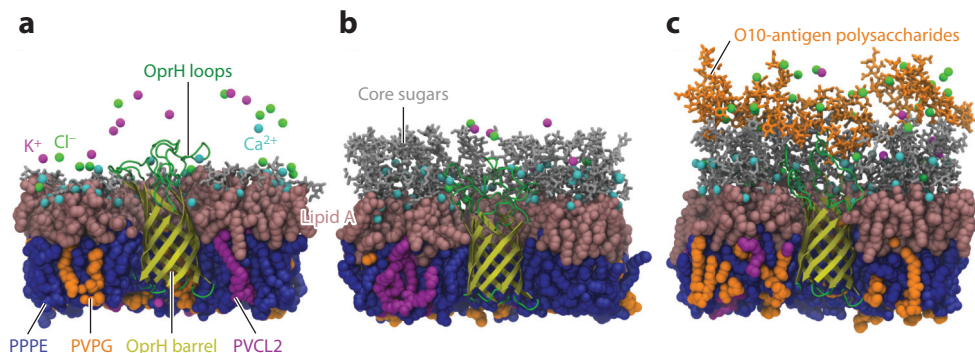


Figure 2

Representative snapshots of OprH embedded in various outer membrane environments with lipopolysaccharide containing (a) only two Kdo residues, (b) G2 core, and (c) G2 core plus two repeating units of O10-antigen (see **Figure 1** for their chemical structures). OprH is shown in ribbon diagrams (yellow for the barrel and green for the loops). Lipid A is represented as pink spheres, core sugars as gray sticks, O10-antigen polysaccharides as orange sticks, PPPE [1-palmitoyl(16:0)-2-palmitoleoyl(16:1 *cis*-9)-phosphatidylethanolamine] as blue spheres, PVPG [1-palmitoyl(16:0)-2-vacenoyleoyl(18:1 *cis*-11)-phosphatidylglycerol] as orange spheres, PVCL2 (1,1'-palmitoyl-2,2'-vacenoyleoyl cardiolipin with a net charge of $-2e$) as magenta spheres, Ca^{2+} as small cyan spheres, K^+ as small magenta spheres, and Cl^- as small green spheres. For clarity, some portion of each system is truncated, and water molecules are not shown. Figure adapted with permission from Reference 42.

chemistry of these systems. The free energies of the permeation of a range of small molecules across the OM were calculated by Carpenter et al. (54). The resulting profiles were found to be distinctly asymmetric. For example, hexane was found to experience a free-energy barrier of ~ 6 kcal/mol on entering the headgroup region of LPS, while no appreciable barrier to its entry into the phospholipid headgroup region was found; the latter observation is due to local lipid reorientation to minimize the energetic penalty for hexane entry. This was followed up with a study of the protein OprD that allows passage of basic amino acids across the OM of *P. aeruginosa* (51). Again, umbrella sampling simulations were performed to calculate the free-energy barriers encountered by arginine as it moves through the protein. Arginine was found to have an energetically favorable location within the polar interior of the protein, whereas for permeation directly across the OM, it would have to overcome an energetic barrier of around 30 kcal/mol. While the correct orientation of arginine has been suggested to be key for translocation through OprD (55), these later simulations also showed that LPS likely plays a role in orienting arginine as it enters the protein vestibule.

The slow diffusion rates of LPS result in limited sampling of the phase space, and thus, while the models are now very accurate, there is a concern about the level of diffusional and/or conformational sampling achievable with standard all-atom molecular dynamics (MD). For example, simulations of the *P. aeruginosa* OM reported by Soares and colleagues (19) required approximately 500 ns for equilibration of deuterium order parameters and area per lipid headgroup. This incomplete or slow sampling issue has necessitated the search for routes to achieve enhanced sampling. One approach has been to employ CG models. Such models have largely been based on the popular MARTINI CG force field. Several different membrane phenomena have been studied using CG models of LPS-containing membranes. Hsu et al. (56) reported a study of the pathways taken by pristine fullerenes to permeate into *E. coli* OM. They showed that under normal conditions (as defined by the study), on the timescale of the simulations, the fullerenes were unable to penetrate beyond the LPS headgroups. However, they were easily able to enter the core of the membranes

from the outer leaflet side at elevated temperatures, when the LPS headgroups were cross-linked by monovalent cations, or if some phospholipids were present in the outer leaflet. Interestingly, once inside the core of the membrane, the fullerenes were not observed to form aggregates, and indeed any aggregates that had formed on the surface of the membrane dissociated once inside the low dielectric region.

A recent study by the Khalid group (50) included five OMPs (BtuB, FhuA, OmpA, OmpX, and EstA) in differing levels of LPS. The simulations showed that each protein has a unique LPS fingerprint, and that furthermore, the patterns of interactions differed for the different levels of LPS considered. For example, for BtuB, if the interactions of charged protein residues with LPS are considered, the greatest number of interactions occurred between lysines in Re-LPS (including only the first two Kdo residues in the core) and between aspartates in Ra-LPS; the number of interactions was comparable between lysines and aspartates when LPS with O-antigen was considered. Another key feature of this study was that even with CG simulations, convergence of properties such as protein tilt angle within the OM can require simulations of approximately 5 μ s. Thus, for equilibrium MD simulations, the slow diffusion of LPS requires far longer simulations to achieve converged behavior than do membranes composed of simpler phospholipids.

Simulation studies of larger, more crowded OM systems have also been reported. Thus far, these have employed simplified OM models (both planar and spherical vesicles), but they have provided novel insights into patterns of molecular interactions within these systems (57–59). For example, the Sansom group (58) simulated \sim 100 copies of *E. coli* OMPs in OM mimetic lipid bilayers (\sim 100-nm length scale) composed of phosphatidylethanolamine (PE) and PG lipids. During the course of the simulations, the OMPs (the TonB-dependent transporter BtuB and the trimeric porin OmpF) were observed to form clusters. The CG simulations were used to parameterize a mesoscale model that was then used to simulate systems of thousands of proteins for timescales of up to 24 μ s. These simulations bring up interesting questions about the membrane localization of OMPs and the role of protein–protein and protein–lipid interactions in regulating the choreography within the OM. For example, it was found that clusters formed only by BtuB tend to be linear in their configuration, whereas those of OmpF were less linear; both proteins engaged in patterns of interactions that are quite different from those observed for multiple copies of G protein–coupled receptors or potassium channels in comparable simulations (Figure 3). Interestingly, a CG study by Shearer & Khalid (47) predicted distinct patterns of behavior to also extend to lipids in the OM. Specifically, cardiolipin clustering was observed in the inner leaflet, directly below regions of low LPS density in the outer leaflet. Thus, the dynamics of lipids and proteins in the OM seems to be more complex than perhaps was anticipated. In the future, it will be interesting to extend such studies of crowded membranes to OM models that incorporate LPS (of various levels) and multiple copy numbers of OMPs in a range of different sizes and oligomeric states to ascertain whether any further patterns of interaction emerge in such complex, crowded systems.

SIMULATING THE INNER MEMBRANE

The IM of Gram-negative bacteria is composed of a mixture of phospholipids including POPE (palmitoyl-oleoyl-phosphatidylethanolamine), POPG (palmitoyl-oleoyl-phosphatidylglycerol), and cardiolipin in various ratios; the precise details of the ratios and headgroup and tail combinations vary from species to species (60–62). Many simulation studies of bacterial IM systems have been conducted over the years. As the parameters of phospholipids have been available for far longer than those of LPS, IM models have more closely resembled the *in vivo* environment for longer than have OM models. Here we focus our attention on a few notable examples of IM simulation studies.

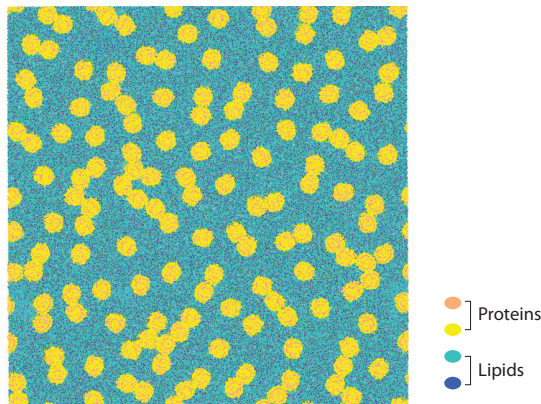


Figure 3

Coarse-grained simulations of a model outer membrane containing multiple copies of the TonB-dependent vitamin B12 transporter BtuB. Distinct clustering behavior is seen. The snapshot was taken after 20 μ s of simulation. The proteins are orange and yellow, and the lipids are cyan and blue. The simulation cell is 110 nm in both the x and y dimensions.

Components of resistance-nodulation-cell division (RND) efflux pumps have been the focus of a number of simulation studies, many of which are reviewed in Reference 63 (**Figure 4**). These pumps are drug/ H^+ antiporters that are fueled by the proton gradient across the IM. They are involved in the recognition and extrusion of a broad range of compounds, including many antibiotics, and thus are of interest from a biomedical perspective as well as basic biophysics. For many years, Ruggerone and Vargiu have led the field by studying the structural dynamics of these protein pumps and its relationship to their function. Here we highlight a few notable examples from their work. A recent simulation study of the *E. coli* antiporter AcrB predicted conformational changes, which lead to the formation of a layer of structured waters on the inner surface of the channel (64). The water layer ensures hydration of the solute moving through the channel and screens the protein-solute interactions to enable transport of the former through the channel. This role of water in the transport process had not previously been considered, so the simulations added to the mechanistic understanding of this protein. In a later study, Ruggerone, Vargiu, and colleagues (65) investigated the molecular origins of the substrate specificity of the transporters AcrB and AcrD via a series of comparative, microsecond-timescale simulations. The substrate binding pockets of both proteins were assessed in terms of a range of metrics, including volume, shape, lipophilicity, electrostatic potential, hydration, and distribution of multifunctional sites. Importantly, they were able to characterize the conformational flexibilities of loops that could also play a role in substrate recognition. Such studies provide invaluable data for drug design that target specific sites. This is important for the RND pumps, as inhibition of their activity is key to combating pathogenic bacteria. In this context, an elegant multidisciplinary study in which X-ray crystallography, atomistic MD simulations, and cell biology assays were employed to characterize the inhibition of AcrB by pyranopyridine derivatives was reported in 2016 by a team of researchers once again including Ruggerone and Vargiu (66). The structural data and simulations were able to provide molecular-level rationalization of the cellular assays. The different studies together showed that pyranopyridines are stabilized within a phenylalanine-rich cage in AcrB, largely through hydrophobic interactions. The molecules studied showed inhibition of the efflux activity of AcrB at lower concentrations than many other molecules that have been proposed as potential inhibitors of RND pumps. Significantly, free-energy calculations enabled

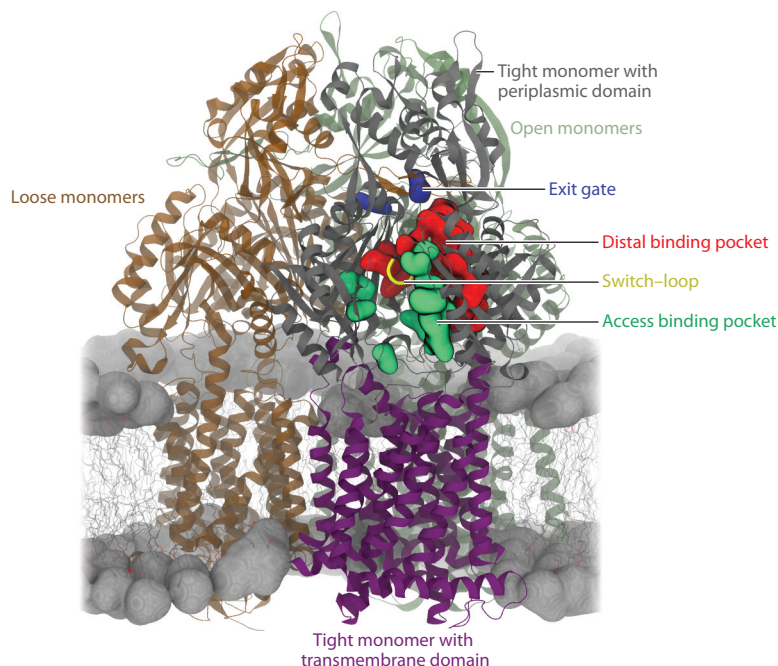


Figure 4

Asymmetric structure of the AcrB protein from *Escherichia coli* embedded in a phospholipid bilayer. Loose and open monomers are represented as brown and dark green ribbons, respectively, while the tight monomer, also shown as ribbons, has pore (periplasmic) and transmembrane domains colored gray and purple, respectively. The main binding pockets (access and distal) are represented as molecular surfaces colored green and red, respectively, while the exit gate is shown in blue. The switch-loop separating the two binding pockets is highlighted in yellow.

the identification of the contributions from the protein, solvent, and ligand molecules to the binding energetics. Thus, each different technique provided a piece of the puzzle, which has helped to build a picture of the mechanism of AcrB inhibition.

Simulation studies of bacterial membrane systems such as the study of AcrB described above, which are performed alongside experimental work, are now becoming de rigueur—new membrane protein structures are now rarely reported without accompanying simulation studies (67–69). Furthermore, studies in which other types of computational methods are combined with simulations and experiments are also becoming more prevalent. For example, sequence coevolution, simulations, cross-linking experiments, and imaging methods were combined to study the twin-arginine protein translocation (Tat) system of *E. coli* (70). The results enabled the identification of protein–protein interactions and led to a structural model for assembly of the active Tat translocase in which substrate binding triggers replacement of TatB by TatA. Another example of combining simulations with experiments is work on YidC insertase from *E. coli*, for example, that was done by Chen and colleagues (71). In this study, *in vivo* cysteine alkylation scanning and MD simulations were used to assess the water accessibility of the protein and its impact on the local membrane environment. Interestingly, the simulations revealed the protein structure to be more compact in the model IM compared to the X-ray structure. This observation once again highlights the importance of considering the local environment when interpreting structural data as well as simulation trajectories.

Recently, Kim et al. (72) used all-atom simulations to investigate the conformational ensemble of lipid II and its elongated forms (lipid VI and lipid XIII) in an IM model and their interactions with penicillin-binding protein 1b (PBP1b, a single-pass transmembrane protein in the IM) from *E. coli*. As the precursor in the peptidoglycan biosynthetic pathway, lipid II carries a nascent peptidoglycan unit that is processed by glycosyltransferases of PBP1b and thus is a target of several classes of antibiotics. Simulations revealed that as the glycan chain grows, the nonreducing end of the nascent peptidoglycan displayed much greater fluctuation along the membrane normal and interacted minimally with the membrane surface. When a nascent peptidoglycan was bound to PBP1b, the stem peptide remained in close contact with PBP1b by structural rearrangement of the glycan chain. Most importantly, this study characterized the number of nascent peptidoglycan units required to reach the transpeptidase domain of PBP1b to be seven or eight. These findings complement experimental results to further understand how the structure of nascent peptidoglycan can dictate the assembly of the peptidoglycan scaffold for bacterial cell wall formation.

SIMULATING THE PERIPLASM

The periplasm is an aqueous region sandwiched between the two membranes of Gram-negative bacteria. Numerous proteins reside either wholly within the periplasm or have some soluble domain within this region while being anchored to either one of the membranes through a transmembrane domain or a membrane anchoring moiety. The cell wall, which is composed of peptidoglycan layers, is also contained within the periplasm.

Simulation studies of some periplasmic proteins have recently been reported. For example, Boags et al. (73) showed the molecular basis for inhibition of LolA by hydrophobic molecules. LolA carries Braun's lipoprotein from the IM across the periplasm and delivers it to LolB, which is anchored to the inner leaflet of the OM. Earlier experimental work had shown that LolA function is inhibited by hydrophobic molecules. Atomistic simulations and free-energy calculations showed that Braun's lipoprotein and the inhibitor form a complex within the cavity of LolA. Atomistic free-energy calculations revealed this complex to have bound less strongly within the LolA cavity than did uncomplexed Braun's lipoprotein. This difference was proposed to be the basis of the inhibition; in other words, the inhibitor does not physically block access to the binding site but instead reduces the strength of the binding between the protein and its natural ligand by forming a complex with the latter.

The modeling and simulation of peptidoglycan provide a rather different challenge due to the structural uncertainty of this biopolymer. While the overall composition of long glycan strands cross-linked by short peptides is largely conserved, some details are still debated, e.g., the arrangement of the strands, as well as the size and shape of the pore-like structures within the mesh. High-resolution microscopy methods, such as work by the Hobbs and Foster groups (74), are now beginning to provide data to clear up some of these uncertainties. Some of the first atomistic-level simulations of the cell wall to provide results comparable to experimental data were those reported by Gumbart et al. (75) in 2014. They constructed a single layer of peptidoglycan, starting with individual residues and building up increasingly larger patches by validating against a range of experimental data (including pore size, elasticity, and thickness) at each expansion stage. Thus, the authors were able to test various possibilities regarding the arrangement of the strands. The agreement between simulations and experiments converged on a model for *E. coli* in which the cell wall is composed predominantly of a single layer of peptidoglycan, with glycan strands aligned in a disordered fashion circumferentially around the cell. Gumbart then followed up this work with simulations combined with experimental work from the Lakey group, on the IMs, OMs, and the cell wall (45). The combined study showed the different responses of

these cell envelope components to surface tension. They produced a model of the distribution of mechanical stress in the *E. coli* cell envelope in which the OM and cell wall share the tension at low turgor pressure (0.3 atm), but tension in the cell wall dominates at high pressure values (>1 atm).

A series of simulations focusing on the cell interactions of OmpA was reported by the Khalid group (39, 76). Having first characterized the conformational dynamics of a model of the dimer formed by the full-length *E. coli* protein OmpA, the group reported simulations of this protein bound to small portions of the peptidoglycan (39). The protein–peptidoglycan complexes were set up using the X-ray structure of the C-terminal domain of OmpA from *Acinetobacter baumannii* (which is bound to a pentapeptide from peptidoglycan, PDB ID 3TD5) (77). The simulations of the full-length *E. coli* OmpA revealed long-lived electrostatic interactions between the soluble C-terminal domain of the protein and the cell wall when the protein is in its monomeric and dimeric forms. It was noted that dimerization reduced the mobility of the C-terminal domains somewhat, and thus the dynamics of the protein in the two oligomeric forms differed. These interactions with the cell wall were further explored in simulations that also included the IM; these are discussed in the following section (78).

PROGRESS IN SIMULATING MULTIPLE COMPONENTS OF THE BACTERIAL CELL ENVELOPE

While above we consider simulations of one component of the cell envelope, the interplay between the different components must be considered to fully understand their dynamic behavior. Recently, such simulation studies and indeed tools to construct these biochemical complex architectures have begun to emerge. In 2019, the first study to incorporate all three components was reported (78). This study simulated OmpA in the OM, Braun's lipoprotein anchored in the OM and covalently bound to the cell wall in periplasm, and TolR in the IM (as well as variations of this combination) at the atomistic level of detail (Figure 5). The results showed that both OmpA and TolR form stable interactions with the cell wall, and that Braun's lipoprotein plays a role in

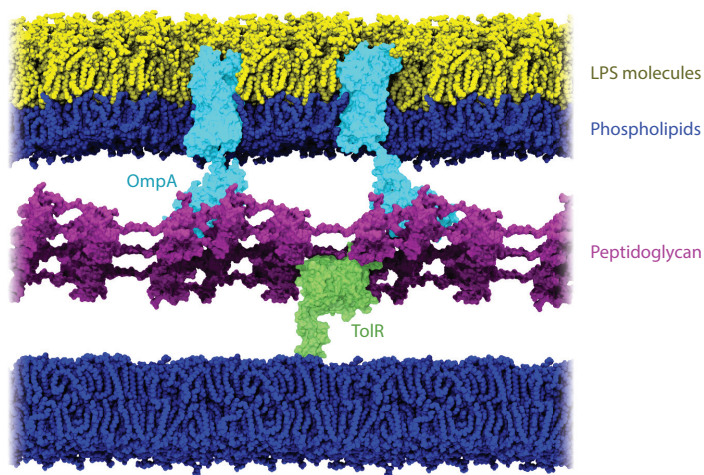


Figure 5

A multicomponent *Escherichia coli* cell envelope system composed of the outer membrane, inner membrane, and a single-layered cell wall (78). Proteins and the cell wall are represented as surfaces; OmpA is cyan, TolR is lime green, and peptidoglycan is purple. LPS molecules are represented as yellow spheres and phospholipids as blue spheres. Abbreviation: LPS, lipopolysaccharide.

facilitating these interactions by tilting and kinking to adjust the width of the periplasmic space. Furthermore, these simulations also showed that the morphology of the cell wall is impacted by the local protein interacting with it. For example, balanced protein–cell wall interactions from the IM and OM sides resulted in a flat cell wall, while protein binding from only one side led to a buckled cell wall. These observations come from simulations of OmpA and Tol only; therefore, further studies, in which other proteins are considered and the cell envelope is more crowded, are necessary to provide additional insights.

The current *Membrane Builder* and *Martini Maker* modules in CHARMM-GUI do allow users to build a membrane system with multiple proteins once these proteins are prearranged in a PDB file. The recent release of the *Multicomponent Assembly* module in CHARMM-GUI has made it easier to build a simulation system with multiple components both with and without phospholipid membranes. When LPS molecules are supported, *Multicomponent Assembly* can be used to model and simulate crowded environments in the OM, thereby moving ever closer to more biologically representative models.

CHALLENGES IN SIMULATING BACTERIAL MEMBRANES

To identify avenues for further work, it is important to consider caveats and limitations of the current state-of-the-art molecular simulations of bacterial membranes. Unsurprisingly, for bacterial membranes these are largely associated with LPS (79). First, few structural data on LPS are available. As mentioned above, there are very few structures of OMPs solved in complex with LPS; thus, an element of educated guesswork is often required when positioning OMPs with respect to LPS within model OMs. Furthermore, when constructing models, asking if it is realistic to assume that the outer leaflet is essentially all LPS is important. Can this be generalized across different bacterial species? The vast majority of experiments that provided estimates of how much LPS is found in the outer leaflet were done over a decade ago, so these likely need to be revisited with modern experimental setups. While LPS is the major component, the OM outer leaflet does contain other complex glycolipids such as the enterobacterial common antigens (ECAs) and capsular polysaccharides (CPSs), whose occurrence is frequently overlooked (80, 81). Therefore, it will be interesting to see the efforts of modeling and simulation of OMs together with LPS, ECAs, and CPSs. On a separate note, encouragingly, experimental work by Lakey, Clifton, and colleagues (82) has led to the development of in vitro asymmetrical, LPS-containing membranes that enable detailed characterization of the physical properties of OM-like membranes, while having tight control over their lipidic compositions. More direct future comparisons between simulations and these experiments will be interesting to see.

In terms of performing MD simulations of the OM, by far the biggest obstacle remains achieving convergence due to the slow diffusion rate of LPS. It was hoped that the smoother energetic landscapes of CG models would significantly enable dynamics; however, this has not been the case with models that use an approximately four to one heavy atom to CG particle mapping. Nevertheless, development of newer CG parameter sets such as MARTINI 3, in which sugars are more accurately represented, does offer more hope for the future. Higher LPS mobility has been achieved at all-atom and CG levels when phospholipids are incorporated into the outer leaflet, which brings us back to the need to quantify the phospholipid content of the OM outer leaflet (56). Sampling of protein–LPS interactions may be enhanced through methods such as replica exchange. Recently, some tests performed by the Khalid group with Hamiltonian replica exchange using CG (MARTINI 2) models, in which the LPS interactions are scaled, have shown that sufficient exchange can be achieved after $\sim 5 \mu\text{s}$ of simulation, in systems without proteins (S. Khalid, unpublished observation). More complex systems are currently being tested. Thus, it seems that using a combination of CG models and enhanced sampling methods may be a route to overcoming slow LPS

diffusion. However, for specific details of protein–LPS interactions, converting the system back to atomistic detail would still be desirable, given the slightly lower resolution of the CG models. So, there is still work to be done to establish protocols for efficient simulations of the OM at multiple levels of resolution. There is good news, however, on setting up simulations of these systems, as the modules within the CHARMM-GUI server provide automated procedures for setting up systems for this purpose. Furthermore, analyses for biomolecular simulations are now generally far less laborious than in the past due to the availability of analysis packages that are code/force field agnostic, such as MDAnalysis (83), as well as more advanced tools with the popular MD codes.

CONCLUSIONS

In conclusion, the literature discussed here, as well as studies to which we have provided references (but were unable to elaborate on due to space limitations), demonstrates the huge strides that have been taken in the last 5 or 6 years in simulations of bacterial membrane systems that are increasingly representative of the *in vivo* environment. Some of the more recent simulation studies that incorporate the cell wall within the periplasm are now enabling the study of the movement of substances across bacterial cell envelope compartments, which represents a step change in simulations of these systems. A particularly gratifying aspect of the state of the bacterial membrane simulation community, and in some ways also a sign of its maturity, is that the models of system components are now available in various force fields and also all-atom and CG levels of detail. The recent progress in large, complex simulation systems has been facilitated primarily by automation of simulation setup, largely led by the Im group, and sharing of parameters through various web servers and repositories. We feel strongly that for future progress, not only should the sharing of parameters/models continue, but so too should frank and open discussions regarding the limitations of current models and methods. In summary, much progress has been made in advancing molecular simulations of not only bacterial membranes, but the whole cell envelope. While there are still issues to be resolved, the progress in enhanced sampling methods, newer CG models, and the availability of greater computing power mean that the future for this field is undoubtedly exciting.

DISCLOSURE STATEMENT

The authors are not aware of any affiliations, memberships, funding, or financial holdings that might be perceived as affecting the objectivity of this review.

ACKNOWLEDGMENTS

This work was supported in part by National Science Foundation grants MCB-1810695 and MCB-1727508, XSEDE MCB-070009, and a Friedrich Wilhelm Bessel Research Award from the Humboldt Foundation (to W.L.), and EPSRC EP/R029407/1, BBSRC BB/H000658/1, and BB/M029573/1 (to S.K.). We thank Seonghoon Kim, Ya Gao, Atilio Vargiu, Paolo Ruggerone, and Mark Sansom for their help in the preparation of this review.

LITERATURE CITED

1. Rev. Antimicrob. Resist. 2014. *Antimicrobial resistance: tackling a crisis for the health and wealth of nations*. Rep., Wellcome Trust, London
2. Yao X, Jericho M, Pink D, Beveridge T. 1999. Thickness and elasticity of Gram-negative murein sacculi measured by atomic force microscopy. *J. Bacteriol.* 181:6865–75

3. Silhavy TJ, Kahne D, Walker S. 2010. The bacterial cell envelope. *Cold Spring Harb. Perspect. Biol.* 2:a000414
4. Erridge C, Bennett-Guerrero E, Poxton IR. 2002. Structure and function of lipopolysaccharides. *Microbes Infect.* 4:837–51
5. Raetz CRH, Whitfield C. 2002. Lipopolysaccharide endotoxins. *Annu. Rev. Biochem.* 71:635–700
6. Lins RD, Straatsma TP. 2001. Computer simulation of the rough lipopolysaccharide membrane of *Pseudomonas aeruginosa*. *Biophys. J.* 81:1037–46
7. Piggot TJ, Holdbrook DA, Khalid S. 2011. Electroporation of the *E. coli* and *S. aureus* membranes: molecular dynamics simulations of complex bacterial membranes. *J. Phys. Chem. B* 115:13381–88
8. Wu EL, Engstrom O, Jo S, Stuhlsatz D, Yeom MS, et al. 2013. Molecular dynamics and NMR spectroscopy studies of *E. coli* lipopolysaccharide structure and dynamics. *Biophys. J.* 105:1444–55
9. Jo S, Wu EL, Stuhlsatz D, Klauda JB, MacKerell AD Jr., et al. 2015. Lipopolysaccharide membrane building and simulation. *Methods Mol. Biol.* 1273:391–406
10. Lee J, Patel DS, Stahle J, Park SJ, Kern NR, et al. 2019. CHARMM-GUI *Membrane Builder* for complex biological membrane simulations with glycolipids and lipoglycans. *J. Chem. Theory Comput.* 15:775–86
11. Wu EL, Cheng X, Jo S, Rui H, Song KC, et al. 2014. CHARMM-GUI *Membrane Builder* toward realistic biological membrane simulations. *J. Comput. Chem.* 35:1997–2004
12. Jo S, Kim T, Iyer VG, Im W. 2008. CHARMM-GUI: a web-based graphical user interface for CHARMM. *J. Comput. Chem.* 29:1859–65
13. Qi YF, Ingolfsson HI, Cheng X, Lee J, Marrink SJ, Im W. 2015. CHARMM-GUI *Martini Maker* for coarse-grained simulations with the Martini force field. *J. Chem. Theory Comput.* 11:4486–94
14. Hsu PC, Bruininks BMH, Jefferies D, de Souza PCT, Lee J, et al. 2017. CHARMM-GUI *Martini Maker* for modeling and simulation of complex bacterial membranes with lipopolysaccharides. *J. Comput. Chem.* 38:2354–63
15. Patel DS, Qi Y, Im W. 2017. Modeling and simulation of bacterial outer membranes and interactions with membrane proteins. *Curr. Opin. Struct. Biol.* 43:131–40
16. Kotra LP, Golemi D, Amro NA, Liu GY, Mobashery S. 1999. Dynamics of the lipopolysaccharide assembly on the surface of *Escherichia coli*. *J. Am. Chem. Soc.* 121:8707–11
17. Soares TA, Straatsma TP. 2007. Towards simulations of outer membrane proteins in lipopolysaccharide membranes. *AIP Conf. Proc.* 963:1375–78
18. Lins RD, Vorpapel ER, Guglielmi M, Straatsma TP. 2008. Computer simulation of uranyl uptake by the rough lipopolysaccharide membrane of *Pseudomonas aeruginosa*. *Biomacromolecules* 9:29–35
19. Soares TA, Straatsma TP, Lins RD. 2008. Influence of the B-band O-antigen chain in the structure and electrostatics of the lipopolysaccharide membrane of *Pseudomonas aeruginosa*. *J. Brazil Chem. Soc.* 19:312–20
20. Soares TA, Straatsma TP. 2008. Assessment of the convergence of molecular dynamics simulations of lipopolysaccharide membranes. *Mol. Simulat.* 34:295–307
21. Kirschner KN, Lins RD, Maass A, Soares TA. 2012. A glycam-based force field for simulations of lipopolysaccharide membranes: parametrization and validation. *J. Chem. Theory Comput.* 8:4719–31
22. Van Oosten B, Harroun TA. 2016. A MARTINI extension for *Pseudomonas aeruginosa* PAO1 lipopolysaccharide. *J. Mol. Graph. Model.* 63:125–33
23. Ma H, Irudayanathan FJ, Jiang W, Nangia S. 2015. Simulating Gram-negative bacterial outer membrane: a coarse grain model. *J. Phys. Chem. B* 119:14668–82
24. Kim S, Patel DS, Park S, Slusky J, Klauda JB, et al. 2016. Bilayer properties of lipid A from various Gram-negative bacteria. *Biophys. J.* 111:1750–60
25. Blasco P, Patel DS, Engstrom O, Im W, Widmalm G. 2017. Conformational dynamics of the lipopolysaccharide from *Escherichia coli* O91 revealed by nuclear magnetic resonance spectroscopy and molecular simulations. *Biochemistry* 56:3826–39
26. Ma HL, Cummins DD, Edelstein NB, Gomez J, Khan A, et al. 2017. Modeling diversity in structures of bacterial outer membrane lipids. *J. Chem. Theory Comput.* 13:811–24
27. Li A, Schertzer JW, Yong X. 2018. Molecular dynamics modeling of *Pseudomonas aeruginosa* outer membranes. *Phys. Chem. Chem. Phys.* 20:23635–48

28. Hughes AV, Patel DS, Widmalm G, Klauda JB, Clifton LA, Im W. 2019. Physical properties of bacterial outer membrane models: neutron reflectometry & molecular simulation. *Biophys. J.* 116:1095–104
29. Baltoumas FA, Hamodrakas SJ, Iconomidou VA. 2019. The Gram-negative outer membrane modeler: automated building of lipopolysaccharide-rich bacterial outer membranes in four force fields. *J. Comput. Chem.* 40:1727–34
30. Gao Y, Lee J, Widmalm G, Im W. 2020. Preferred conformations of lipooligosaccharides and oligosaccharides of *Moraxella catarrhalis*. *Glycobiology* 30:86–94
31. Straatsma TP, Soares TA. 2009. Characterization of the outer membrane protein OprF of *Pseudomonas aeruginosa* in a lipopolysaccharide membrane by computer simulation. *Proteins Struct. Funct. Bioinform.* 74:475–88
32. Piggot TJ, Holdbrook DA, Khalid S. 2013. Conformational dynamics and membrane interactions of the *E. coli* outer membrane protein FecA: a molecular dynamics simulation study. *Biochim. Biophys. Acta* 1828:284–93
33. Holdbrook DA, Piggot TJ, Sansom MS, Khalid S. 2013. Stability and membrane interactions of an auto-transport protein: MD simulations of the Hia translocator domain in a complex membrane environment. *Biochim. Biophys. Acta* 1828:715–23
34. Wu EL, Fleming PJ, Yeom MS, Widmalm G, Klauda JB, et al. 2014. *E. coli* outer membrane and interactions with OmpLA. *Biophys. J.* 106:2493–502
35. Berglund NA, Piggot TJ, Jefferies D, Sessions RB, Bond PJ, Khalid S. 2015. Interaction of the antimicrobial peptide polymyxin B1 with both membranes of *E. coli*: a molecular dynamics study. *PLOS Comput. Biol.* 11:e1004180
36. Fleming PJ, Patel DS, Wu EL, Qi Y, Yeom MS, et al. 2016. BamA POTRA domain interacts with a native lipid membrane surface. *Biophys. J.* 110:2698–709
37. Balusek C, Gumbart JC. 2016. Role of the native outer-membrane environment on the transporter BtuB. *Biophys. J.* 111:1409–17
38. Ortiz-Suarez ML, Samsudin F, Piggot TJ, Bond PJ, Khalid S. 2016. Full-length OmpA: structure, function, and membrane interactions predicted by molecular dynamics simulations. *Biophys. J.* 111:1692–702
39. Samsudin F, Ortiz-Suarez ML, Piggot TJ, Bond PJ, Khalid S. 2016. OmpA: a flexible clamp for bacterial cell wall attachment. *Structure* 24:2227–35
40. Patel DS, Re S, Wu EL, Qi Y, Klebba PE, et al. 2016. Dynamics and interactions of OmpF and LPS: influence on pore accessibility and ion permeability. *Biophys. J.* 110:930–38
41. Hsu PC, Samsudin F, Shearer J, Khalid S. 2017. It is complicated: curvature, diffusion, and lipid sorting within the two membranes of *Escherichia coli*. *J. Phys. Chem. Lett.* 8:5513–18
42. Lee J, Patel DS, Kucharska I, Tamm LK, Im W. 2017. Refinement of OprH-LPS interactions by molecular simulations. *Biophys. J.* 112:346–55
43. Jefferies D, Hsu PC, Khalid S. 2017. Through the lipopolysaccharide glass: A potent antimicrobial peptide induces phase changes in membranes. *Biochemistry* 56:1672–79
44. Matthias KA, Strader MB, Nawar HF, Gao YS, Lee J, et al. 2017. Heterogeneity in non-epitope loop sequence and outer membrane protein complexes alters antibody binding to the major porin protein PorB in serogroup B *Neisseria meningitidis*. *Mol. Microbiol.* 105:934–53
45. Hwang H, Paracini N, Parks JM, Lakey JH, Gumbart JC. 2018. Distribution of mechanical stress in the *Escherichia coli* cell envelope. *Biochim. Biophys. Acta Biomembr.* 1860:2566–75
46. Lee J, Pothula KR, Kleinekathöfer U, Im W. 2018. Simulation study of Ock5 functional properties in *Pseudomonas aeruginosa* outer membranes. *J. Phys. Chem. B* 122:8185–92
47. Shearer J, Khalid S. 2018. Communication between the leaflets of asymmetric membranes revealed from coarse-grain molecular dynamics simulations. *Sci. Rep.* 8:1805
48. Ma HL, Khan A, Nangia S. 2018. Dynamics of OmpF trimer formation in the bacterial outer membrane of *Escherichia coli*. *Langmuir* 34:5623–34
49. Kesireddy A, Pothula KR, Lee J, Patel DS, Pathania M, et al. 2019. Modeling of specific lipopolysaccharide binding sites on a Gram-negative porin. *J. Phys. Chem. B* 123:5700–8
50. Shearer J, Jefferies D, Khalid S. 2019. Outer membrane proteins OmpA, FhuA, OmpF, EstA, BtuB, and OmpX have unique lipopolysaccharide fingerprints. *J. Chem. Theory Comput.* 15:2608–19

51. Samsudin F, Khalid S. 2019. Movement of arginine through OprD: the energetics of permeation and the role of lipopolysaccharide in directing arginine to the protein. *J. Phys. Chem. B* 123:2824–32
52. Golla VK, Sans-Serramitjana E, Pothula KR, Benier L, Bafna JA, et al. 2019. Fosfomycin permeation through the outer membrane porin OmpF. *Biophys. J.* 116:258–69
53. Bhamidimarri SP, Zahn M, Prajapati JD, Schleberger C, Soderholm S, et al. 2019. A multidisciplinary approach toward identification of antibiotic scaffolds for *Acinetobacter baumannii*. *Structure* 27:268–80
54. Carpenter TS, Parkin J, Khalid S. 2016. The free energy of small solute permeation through the *Escherichia coli* outer membrane has a distinctly asymmetric profile. *J. Phys. Chem. Lett.* 7:3446–51
55. Parkin J, Khalid S. 2014. Atomistic molecular-dynamics simulations enable prediction of the arginine permeation pathway through OccD1/OprD from *Pseudomonas aeruginosa*. *Biophys. J.* 107:1853–61
56. Hsu PC, Jefferies D, Khalid S. 2016. Molecular dynamics simulations predict the pathways via which pristine fullerenes penetrate bacterial membranes. *J. Phys. Chem. B* 120:11170–79
57. Holdbrook DA, Huber RG, Piggot TJ, Bond PJ, Khalid S. 2016. Dynamics of crowded vesicles: local and global responses to membrane composition. *PLOS ONE* 11:e0156963
58. Chavent M, Duncan AL, Rassam P, Birkholz O, Helie J, et al. 2018. How nanoscale protein interactions determine the mesoscale dynamic organisation of bacterial outer membrane proteins. *Nat. Commun.* 9:2846
59. Fowler PW, Helie J, Duncan A, Chavent M, Koldso H, Sansom MS. 2016. Membrane stiffness is modified by integral membrane proteins. *Soft Matter* 12:7792–803
60. Vance DE, Vance JE. 2002. *Biochemistry of Lipids, Lipoproteins, and Membranes*. Amsterdam: Elsevier
61. Shokri A, Larsson G. 2004. Characterisation of the *Escherichia coli* membrane structure and function during fedbatch cultivation. *Microb. Cell Fact.* 3:9
62. Raetz CR. 1978. Enzymology, genetics, and regulation of membrane phospholipid synthesis in *Escherichia coli*. *Microbiol. Rev.* 42:614–59
63. Vargiu AV, Ramaswamy VK, Malloci G, Malvacio I, Atzori A, Ruggerone P. 2018. Computer simulations of the activity of RND efflux pumps. *Res. Microbiol.* 169:384–92
64. Vargiu AV, Ramaswamy VK, Malvacio I, Malloci G, Kleinekathöfer U, Ruggerone P. 2018. Water-mediated interactions enable smooth substrate transport in a bacterial efflux pump. *Biochim. Biophys. Acta Gen. Subj.* 1862:836–45
65. Ramaswamy VK, Vargiu AV, Malloci G, Dreier J, Ruggerone P. 2017. Molecular rationale behind the differential substrate specificity of bacterial RND multi-drug transporters. *Sci. Rep.* 7:8075
66. Sjuts H, Vargiu AV, Kwasny SM, Nguyen ST, Kim HS, et al. 2016. Molecular basis for inhibition of AcrB multidrug efflux pump by novel and powerful pyranopyridine derivatives. *PNAS* 113:3509–14
67. Hughes GW, Hall SCL, Laxton CS, Sridhar P, Mahadi AH, et al. 2019. Evidence for phospholipid export from the bacterial inner membrane by the Mla ABC transport system. *Nat. Microbiol.* 4:1692–705
68. Pathania M, Acosta-Gutierrez S, Bhamidimarri SP, Basle A, Winterhalter M, et al. 2018. Unusual constriction zones in the major porins OmpU and OmpT from *Vibrio cholerae*. *Structure* 26:708–21.e4
69. Abellon-Ruiz J, Kaptan SS, Basle A, Claudi B, Bumann D, et al. 2017. Structural basis for maintenance of bacterial outer membrane lipid asymmetry. *Nat. Microbiol.* 2:1616–23
70. Alcock F, Stansfeld PJ, Basit H, Habersetzer J, Baker MAB, et al. 2016. Assembling the Tat protein translocase. *eLife* 5:e20718
71. Chen YY, Capponi S, Zhu L, Gellenbeck P, Freites JA, et al. 2017. YidC insertase of *Escherichia coli*: water accessibility and membrane shaping. *Structure* 25:1403–14
72. Kim S, Pires MM, Im W. 2018. Insight into elongation stages of peptidoglycan processing in bacterial cytoplasmic membranes. *Sci. Rep.* 8:17704
73. Boags A, Samsudin F, Khalid S. 2019. Details of hydrophobic entanglement between small molecules and Braun's lipoprotein within the cavity of the bacterial chaperone LolA. *Sci. Rep.* 9:3717
74. Turner RD, Mesnage S, Hobbs JK, Foster SJ. 2018. Molecular imaging of glycan chains couples cell-wall polysaccharide architecture to bacterial cell morphology. *Nat. Commun.* 9:1263
75. Gumbart JC, Beeby M, Jensen GJ, Roux B. 2014. *Escherichia coli* peptidoglycan structure and mechanics as predicted by atomic-scale simulations. *PLOS Comput. Biol.* 10:e1003475
76. Samsudin F, Boags A, Piggot TJ, Khalid S. 2017. Braun's lipoprotein facilitates OmpA interaction with the *Escherichia coli* cell wall. *Biophys. J.* 113:1496–504

77. Park JS, Lee WC, Yeo KJ, Ryu KS, Kumarasiri M, et al. 2012. Mechanism of anchoring of OmpA protein to the cell wall peptidoglycan of the gram-negative bacterial outer membrane. *FASEB J.* 26:219–28
78. Boags AT, Samsudin F, Khalid S. 2019. Binding from both sides: TolR and full-length OmpA bind and maintain the local structure of the *E. coli* cell wall. *Structure* 27:713–24.e2
79. Parkin J, Chavent M, Khalid S. 2015. Molecular simulations of Gram-negative bacterial membranes: a vignette of some recent successes. *Biophys. J.* 109:461–68
80. Kuhn HM, Meier-Dieter U, Mayer H. 1988. ECA, the enterobacterial common antigen. *FEMS Microbiol. Rev.* 4:195–222
81. Whitfield C. 2006. Biosynthesis and assembly of capsular polysaccharides in *Escherichia coli*. *Annu. Rev. Biochem.* 75:39–68
82. Clifton LA, Holt SA, Hughes AV, Daulton EL, Arunmanee W, et al. 2015. An accurate in vitro model of the *E. coli* envelope. *Angew. Chem.* 54:11952–55
83. Michaud-Agrawal N, Denning EJ, Woolf TB, Beckstein O. 2011. MDAAnalysis: a toolkit for the analysis of molecular dynamics simulations. *J. Comput. Chem.* 32:2319–27